Available online at www.sciencedirect.com

SciVerse ScienceDirect

journal homepage: http://www.elsevier.com/locate/rpor

Original research article

Monte Carlo characterizations mapping of the (γ,n) and (n,γ) photonuclear reactions in the high energy X-ray radiation therapy

*Hosein Ghiasi**

University of Medical Sciences, Department of Medical Physics, Iran

ARTICLE INFO

Article history:
Received 6 February 2013
Received in revised form
13 April 2013
Accepted 7 July 2013

Keywords:
Photoneutron
Monte Carlo
Shielding
Capture gamma ray

ABSTRACT

Aim: The aim of this work was to map the characteristics of (n,γ) and (γ,n) reactions in a high energy photon radiation therapy.

Background: Photoneutrons produced in the high energy X-Ray radiation therapy may damage patients and staff. It is due to high RBE of the produced neutrons according to their energy and isotropic emission. Characterization of the photoneutrons can help us in appropriate shielding.

Materials and methods: This study focused on the photoneutron and capture gamma ray phenomena. Characteristics such as dose value, fluence and spectra of both the neutrons and the by produced prompt gamma ray were described.

Results and discussion: Neutron and prompt gamma spectra in different points showed the neutrons to be thermalized when increasing the distance from the linac. Energy of the neutrons changed from about 0.6 MeV at the isocentre to around 10^{-08} MeV at the outer door position. Although the neutrons were found as fast neutrons, their spectra showed they were thermal neutrons at the outer door position. Additionally, it was seen that the energy of the gamma rays is higher than the scattered X-ray energy. The energy of gamma rays was seen to be up to 10 MeV while the linac photons had energy lower than 1 MeV. Neutron source strength obtained in this work was in good agreement with the published data, which may be a confirmation of our simulation accuracy.

Conclusion: The study showed that the Monte Carlo simulation can be applied in the radiotherapy and industrial radiation works as a useful and precise estimator. We also concluded that the dose from the prompt gamma ray at the outer door location is higher than the scattered radiation from the linac and should be considered in the shielding.

* Tel.: +98 4127292564; fax: +98 04127292564.
E-mail addresses: hoseinghiasi62@gmail.com, h_ghyasy@yahoo.com

1507-1367/$ – see front matter © 2013 Greater Poland Cancer Centre. Published by Elsevier Urban & Partner Sp. z o.o. All rights reserved.
http://dx.doi.org/10.1016/j.rpor.2013.07.003

1. Background

Photonuclear reactions become important in the X-Ray radiation therapies with energies higher than 8–10 MV[1]. When a photon has energy higher than the threshold energy of reaction (7–10 MeV), secondary particles emission can occur[2]. Giant dipole resonance (GDR) in which the target material nucleus undergoes instability in the nucleus energy levels is the cause for the secondary particles emission by the nucleus to achieve a stable energy state. The emitted particle may be a neutron, proton, alpha particle and heavy ions[3–5]. However, the neutrons are uncharged and are not absorbed with the LINAC head materials[6]. And this is the key why we study only photoneutrons? For this substantial matter, photoneutron production is a concern and a problem in terms of radiation protection. For example, a proton is absorbed at several millimeters away from the produced origin because of its electrical charge and the Columbus reaction[7]. However, a produced photoneutron is able to go to the maze and outside of the treatment room. The propagation of photoneutrons in the treatment room can lead to an increase in the patients' and staff's exposure to dose equivalent[8–11]. Useful beams and the entire room and maze are contaminated with photoneutron production. Patient body and organs may be a source of photoneutron production and the produced neutrons may be absorbed in or outside of the patient's body. On the other hand, the photoneutrons are produced in a range of energy associated with higher radiobiological damages[3]. The radiobiological effects were reported to be up to 20 times higher those of a photon with any energy[3]. Secondary malignancies reported as the late effects of the produced photoneutrons and capture gamma.

2. Aim

These hazardous effects of neutrons in a high energy radiation therapy were the reason to perform this study and mapping the characteristics of the secondary photoneutrons produced and gamma rays. In this study, we tried to characterize the secondary photoneutrons produced and consequent capture gamma rays.

3. Materials and methods

MCNPX code of the Monte Carlo (MC)[12] method was used in the entire the study. The code has capabilities such as to simulate very complex and rolled geometries. Additionally, physical phenomena such as photon–neutron–electron and coupled particles transport can be achieved using the code and its data libraries. With the usage of the code, Varian 2100 Clinac geometry and physical aspects of the LINAC were simulated according to the manufacturer provided data. Our modeling was validated in our previous works. A typical treatment room according to International Atomic Energy Agency (IAEA No. 47)[1] recommendation on the radiotherapy facilities designing was simulated, made of ordinary concrete. Running the simulated program for short times, BNUM (which controls the number of photons produced per incident primary electron) of electron phys card was optimized and the number of 5 was attributed to the BNUM value. Then, code for any primary electron, transports 5 photons per initial primary incident electron and reduces the running time more than 14 times and statistical error around 1.86 times. With inserted other variance reduction options, produced neutrons energy, fluence, flux, spectra and dose equivalent in different points in the simulated room were scored using different tallies. Photon, neutron and neutron capture gamma ray characteristics were tallied in the isocentre and different points at the isocentre plane, in the room and position of the inside and outside of the maze door. For this, tally of F4 in an air filled spherical cell in diameter of 1 cm was applied and tallied the particles per cm^2. Obtained results were discussed and compared with the published data and commissioned. Dose equivalent was scored in water filled small spherical cell inside and outside of the door and also at the isocentre. Additionally, we calculated and compared the photoneutrons and capture gamma ray dose equivalent using the method we proposed in our previous work. Other analytical methods were used to compare the data, such as Kersey, French, McCall and Wu-McGinley methods[13–17]. The shielding performance and the results were evaluated and the results discussed. In the previous work[18] we proposed an analytical method and sensitized the analytical methods to walls and room material compositions. In this work, we tried to evaluate the proposed methods. Additionally, full mapping of the photoneutron and capture gamma ray characteristics was done in the context of the radiological protection issues.

4. Results and discussion

The results of this work were presented in several sections. The first section presents our results and some discussions on the photoneutron, photon and neutron capture gamma ray spectra. The trend of the spectra with differing distance is discussed. Published data on the neutron, gamma and LINACs photon spectra were considered and discussed. A good agreement was found between the published data and our results in dosed, fluence and spectra in this section. Obtained data is close to the results in the literature. The results and comparisons are presented in the tables.

4.1. *Spectra (photon, neutron, gamma)*

Figs. 2–4 show photoneutron spectra at the isocentre, point A and maze door position. Fig. 5 also shows the neutron spectra outside the door. The two Figs. 6 and 7 show the spectra of neutron at the primary and secondary barrier positions. Door modification is obviously seen from the spectra at the outside of the door. It is shown in Fig. 2 that the fast portion of the photoneutrons is dominant at the isocentre. From an analytical characterization of the photoneutrons at the point it can be deduced that about 89% of the produced neutrons are thermal neutrons with lower energy and unfortunately highest biological effect among the other energies of neutrons. Eq. (1) defines photoneutrons distribution and its thermal and fast components. First term is thermal portion and the second

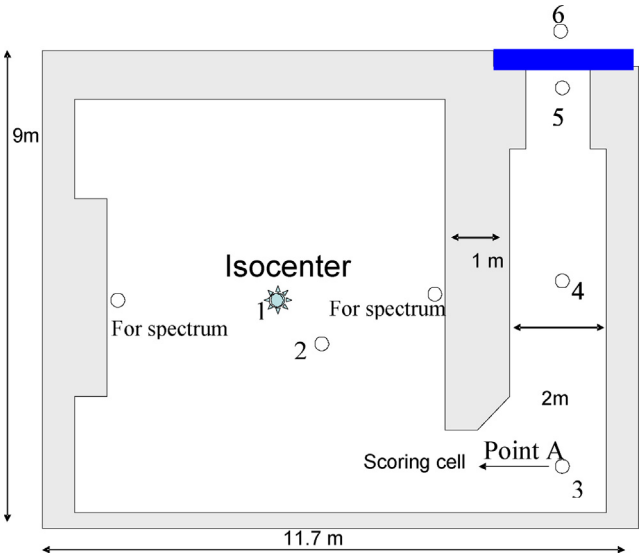

Fig. 1 – A top view of the simulated room and the points in the room that doses, fluence and spectra were calculated. (Point A was shown in the figure).

term shows the fast neutrons reported by Tossi et al[19].

$$\frac{dN}{dE_n} = \frac{0.8929E_n}{(0.5)^2}\exp\left(\frac{-E_n}{0.5}\right) + \frac{0.1071\ln[E_{max}/E_n + 7.34]}{\int_0^{E_{max}-7.34}\ln[E_{max}/E_n + 7.34]dE_n} \quad (1)$$

Only 11% of the neutrons are epithermal and fast. On the other hand, the spectrum shows that more than 2 MeV neutrons are negligible and have any portion at the spectrum. There are two main peaks, around 600–700 KeV, and the other at the 1.2 MeV energy. Lower the energy, higher the radiobiological effects but not all. At the point A (the point of inner entrance of treatment room which is at the distance of 120 cm from the wall) in Fig. 1, the thermal portion of the photoneutron increases and epithermal and fast neutrons decrease. But at the maze door, a dominant portion of the spectrum is taken by thermal neutrons and for this reason detection of the neutron is hard. Energy associated with the neutron is around 10^{-08} MeV.

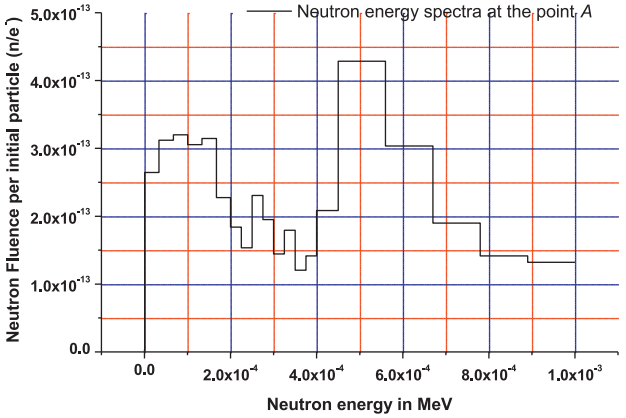

Fig. 2 – Neutron spectra at the 100 cm from the linac tungsten target or X-ray production point (point 2 in Fig. 1).

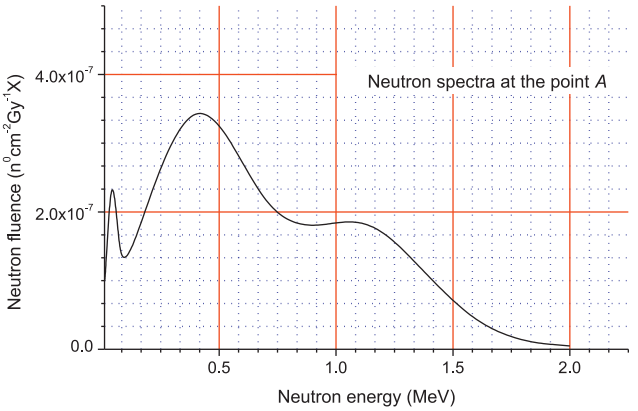

Fig. 3 – Derived photoneutron spectra at the point 3 (point A in the text) at the inner maze entrance.

The peak lies out in the thermal region of the neutron energy. Tremendous hazards would potentially exist if the maze door was not designed in the radiation treatment rooms. Isotropic emission of the photoneutrons leads to a whole buy radiation received by the staff and patient from the photoneutrons. Published data support our results and our modeling. Capture gamma ray spectrum at the maze entrance and linac photon spectrum were mapped in Figs. 5 and 6, respectively. It is seen that capture gamma ray is higher than linac photons at the maze entrance. Linac produced photoneutron spectra shape for all energies are the same despite energy difference of linacs. Although the altitude is different, the shape of the spectra is constant. Capture gamma ray spectrum and linac photon spectrum also were mapped in Fig. 8.

4.2. *Neutron source strength*

In the photoneutron and capture gamma ray calculations a parameter called linac neutron source strength plays an important role. It was defined as "the number of neutrons produced by LINAC while delivering 100 cGy dose from photon to the isocentre in water phantom". The LINAC source

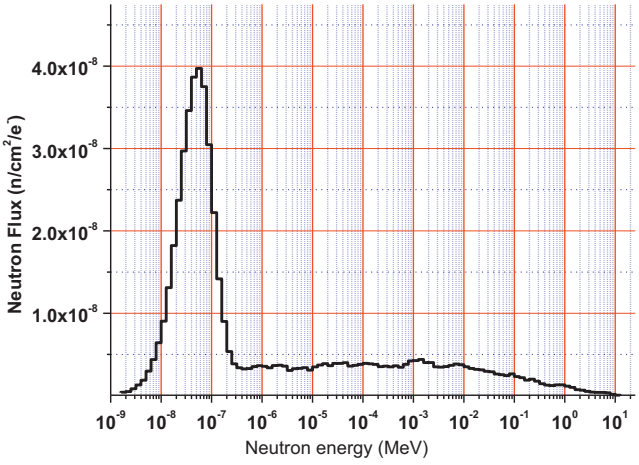

Fig. 4 – Obtained spectra of the photoneutrons at the maze entrance. The energy peak is at 10^{-8} Mev and fast neutrons are very low or negligible.

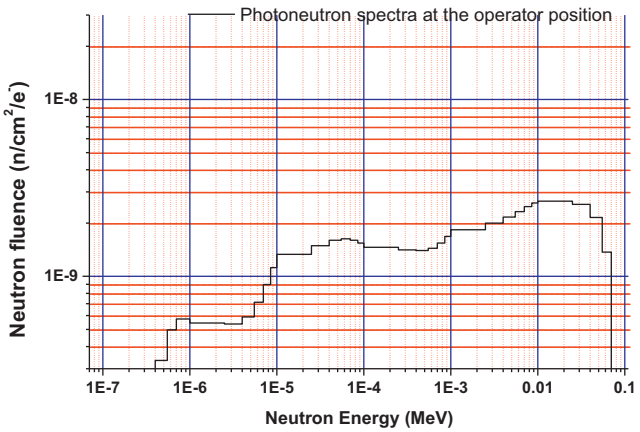

Fig. 5 – Photoneutron spectra outside of the outer entrance door of maze (point 6). The spectra show the door modification on the neutrons energy.

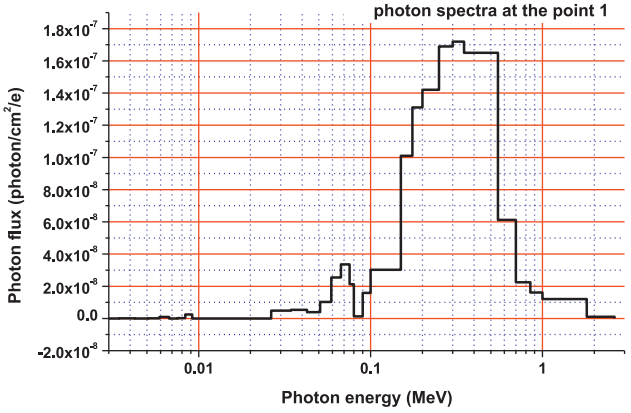

Fig. 6 – Photoneutron spectra derived at the primary barrier position.

strength number is based on dose per initial particle calculations in case of the neutron and gamma ray. Different numbers were reported for different machines and energies. For our simulated machine, Varian 2100 Clinac operating in 18 MV, 1.2×10^{12} neutron per photon Gy at the isocentre was reported in different reports[1]. But, in our previous work, we obtained the value as 1.3×10^{12}. The difference with our report

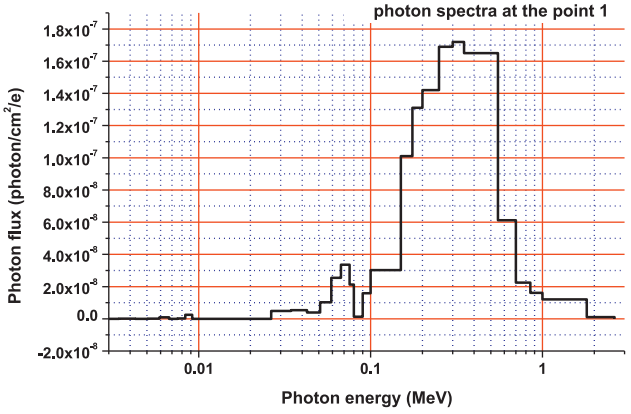

Fig. 7 – photoneutron spectra derived at the secondary barrier.

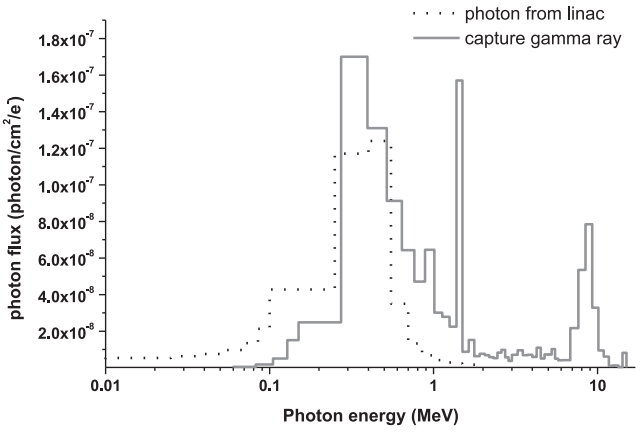

Fig. 8 – Neutron capture gamma ray and LINACs photons spectra at the outer maze entrance. Capture gamma ray is dominant.

and other calculations can be attributed to the fact that we calculated it in the room, while others, such as the manufacturers, calculated it in open air. Its definition also does not consider room. We stated that the value is for room + LINAC. Then, we considered room produced neutrons, too, in our calculations. It can be deduced from this difference that around 1×10^{11} neutrons per Gy at the isocentre is due to room production of photoneutron[20]. Other values for the neutron source strength were reported. The reported values are $0.9–1.2 \times 10^{12}$. Our calculated value in this work is in good agreement with the values reported for the Varian Clinac operating at 18 MV. We calculated the crossing neutrons per initial electron in program running. Then, we calculated the number of electrons with the strongest impact on the target for delivering 100 cGy to the isocentre. Using this data, Qn or neutron source strength was calculated as 1.3×10^{12}. Our calculations were inside the concrete room and walls produced neutrons also considered in Q_N. Analytical method describing the Q_N is as below[19]:

$$\varphi'_A = \frac{(Q_N + Q_W)}{4\pi d^2} + \frac{5.4 \times (Q_N + Q_W)}{2\pi S} + \frac{1.26 \times (Q_N + Q_W)}{2\pi S} \quad (2)$$

From Eq. (2), it can be seen that both fast and thermal neutrons contribute to the Q_N calculation. Q_w is the room produced neutron source strength. This value must be calculated at 100 cm from target. On the other hand, it can be found out from the equation that the fast neutrons decline with r^{-2}. However, thermal neutrons related to the room surface not distance from the target. We used a full simulated linac model for deriving the data instead of a simplified model. Because in the simulated model many physical phenomena are omitted, such as the relation between field size and output fluence. Table 1 shows our obtained Q_N and those from other studies. In the published literature 18 MV linac neutron source strength is around 1.2×10^{12} neutrons per gray at the isocentre.

4.3. *Fluence and flux*

IAEA safety report number 47 stated that for units operating above 10 MV the neutron fluence must be considered. F4 tally

Table 1 – Photoneutron dose equivalent at different locations at the simulated room with both the MC and analytical methods in mSv per Gy of X-ray at the isocentre.

Point	Mean analytical results in mSv Gy^{-1}	Dose equivalent mSv Gy^{-1}	Mean analytical results in mSv Gy^{-1} this study	Dose equivalent (mSv Gy^{-1}) in this study
1 (isocentre)	6.90×10^{-1}	5.41×10^{-1}	6.20×10^{-1}	5.45×10^{-1}
2 (1 m from isocentre)	3.10×10^{-1}	2.67×10^{-1}	3.65×10^{-1}	2.77×10^{-1}
3	9.60×10^{-2}	8.54×10^{-2}	9.12×10^{-2}	8.50×10^{-2}
4	8.54×10^{-3}	6.74×10^{-3}	8.39×10^{-3}	7.71×10^{-3}
5 (50 cm inner the entrance door)	3.16×10^{-3}	2.16×10^{-3}	3.90×10^{-3}	1.56×10^{-3}
6 (50 cm outer the door)	n/a	n/a	2.89×10^{-3}	9.65×10^{-5}

Table 2 – The reported results (published data) and our results in the neutron source strength calculation.

Linac model	Operating energy (MV)	Neutron source strength ($\times 10^{12}$)	References
Varian 2300 C/D linac	18	0.95	Followill et al. (2003)
Varian 2100 Clinac	18	0.96	Followill et al. (2003)
Varian 2100 Clinac	18	0.87	Followill et al. (2003)
Varian 2100 Clinac	18	1.3	Mesbahi et al. (2010)
This study	18	1.3	*
Varian 1800 linac	18	1.22	IAEA no 47

positioned in a spherical cell whose location is in the isocentre and maze entrance, primary and secondary barrier positions, and point A. With very small beams of energy an accurate spectra was obtained. Neutron and gamma ray fluence was simulated and calculated at the isocentre. Table 2 shows the results and comparison between the literature and our results in terms of the neutron source strength calculation. The result is a validation of our simulation of the linac. We found the fluence of neutrons at the isocentre as 1.09×10^7 neutrons per ray of isocentre dose. Kase et al.[20] also found same value with simulation of the same machine. Other literature sources also reported the values close to our result. At the maze entrance, our result was 3×10^{-8} neutrons per Gy. Analytical methods reported for calculating the neutron fluence at the point of interest (d):

$$\Phi_d = \frac{Q_N}{4\pi d^2} \quad (3)$$

Eq. (3) shows fast neutrons following from the inverse square law. Increasing the distance from the target (d), decreases the fast neutrons fluence.

Thermal fluence obeys Eq. (4):

$$\Phi_{th} = \frac{5.4Q_N}{2\pi S} + \frac{1.26Q_N}{2\pi S} \quad (4)$$

These equations only calculate the linac produced neutron fluence, but room produced neutrons can be calculated from Eq. (2).

Our MC results were in good agreement with the analytical calculation formulas. Difference was around 8% and it is good agreement. From the equations, it can be found out that the neutron fluence depends on energy, linac model, room design and total room surface. Additionally, it is independent from workload of the linac. Naseri and Mesbahi[20] made a review of photoneutron production in high energy radiation therapy.

4.4. *Dose equivalent*

Photoneutron and capture gamma ray dose equivalent was tallied using F6 tally of MCNPX code of MC. Neutron dose was tallied at 100 cm from the target and was compared with the literature results. Capture gamma ray dose equivalent was calculated at the maze entrance as well as neutron dose equivalent. A water filled spherical cell 0.5 cm in diameter was positioned at the isocentre compromising the statistical error and dose resolution, in the maze entrance the cell diameter increased to 1 cm. All of the calculations concerning neutrons were with 2% statistical error, but in the case of photon or gamma the error was less than 0.8%. The results we found in points 1–6 are shown in Table 1. Ref. 21 reported dose equivalent at the isocentre as 1.843×10^{-3} and 0.169×10^{-3} mSv Gy^{-1}. McGinley and Landry studied on the Varian 18 MV machine and found dose to two machine and beams. Chen et al. used FLUKA and bobble detector (BD) and studied the neutron ambient dose in several locations. The difference between our result and published results is low showing our modeling is sufficiently accurate. On the other hand, we calculated the neutron and gamma ray with analytical methods. Among the methods, the Wu-McGinley method was in the best agreement with MC results. Table 1 shows the results. Fig. 9 shows dose equivalent in each 20 cm at the maze calculated with all of the methods. From the figure, Wu-McGinley shows good agreement with MC method. The other methods often overestimate the dose according to Fig. 10. Fig. 9 shows a comparison between the analytical methods and MC simulation.[22–27]

4.5. *Door performance*

Maze door causes moderation of the photoneutron characteristics. Value of dose and spectrum was moderated with the maze lead and paraffin door. Inside and outside of the door, neutron spectrum was mapped and compared. The door reduces the neutrons highly and sufficiently. Fig. 7 shows a comparison between inside and outside of locked door.

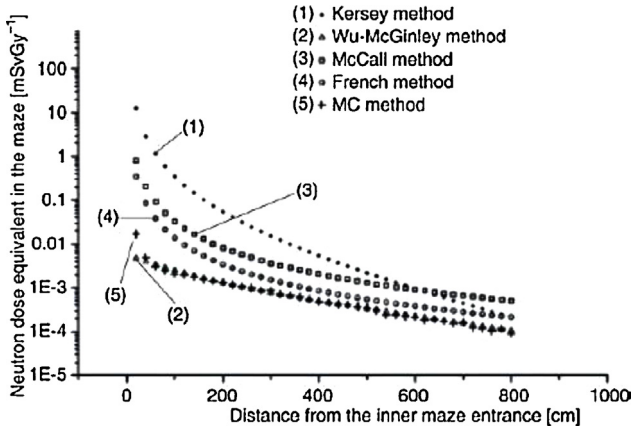

Fig. 9 – Comparison of calculated neutron dose equivalents between analytical methods and MC method.

Additionally, IAEA recommended maximum acceptable weakly dose was met using the program and physical aspects of the simulations.

5. Conclusions

Our conclusion from the work was that the photoneutron calculation and simulation results are close to each other. If the time consuming feature of MC method could be solved it would be predominant of other methods. In conclusion, we summarized features and superiority over the other methods:

- Although it is time consuming, the results of it is accurate in macro and nano scales.
- When solving a radiation problem, the operator does not receive any radiation dose while the results are accurate.
- It is easy to design a favorite room without any workers and architecture and without any radiation. In designing a room trial and error cannot occur, but in the MC method it is feasible.
- Data in the package of MC are obtained in a reliable method and organization in Los Alamos. Then in cases when experimental work is not possible, the MC method can offer us reliable data.

Conflict of interest

None declared.

Financial disclosure

None declared.

REFERENCES

1. International Atomic Energy Agency (IAEA). Radiation protection in the design of radiotherapy facilities. In: *Safety Reports series No. 47*. Vienna: IAEA; 2006.
2. Mc Ginley PH, Butker EK. Evaluation of neutron dose equivalent levels at the maze entrance of medical accelelator treatment rooms. *Med Phys* 1990;**18**:279–81.
3. NCRP. *NCRP Report 116. Limitation of exposure to ionizing radiation*. Bethesda, MD: National Council on Radiation Protection and Measurements; 1993.
4. McCall RC. *Neutron yield of medical electron accelerators. SLAC-PUB 4480*. Stanford, CA: Stanford Linear Accelerator Center; 1987.
5. Zanini A, Durisi E, Fasolo F, et al. Monte Carlo simulation of the photoneutron field in linac radiotherapy treatments with different collimation systems. *Phys Med Biol* 2004;**49**: 571–82.
6. Howell RM, Ferenci MS, Hertel NE, Fullerton GD. Investigation of secondary neutron dose for 18 MeV dynamic MLC IMRT delivery. *Med Phys* 2005;**32**(3):786–93.
7. Mao XS, Kase KR, Liu JC, Nelson WR, Kleck JH, Johnsen S. Neutron sources in the Varian Clinac 2100 C/2300 C medical accelerator calculated by the EGS4 code. *Health Phys* 1997;**72**:524–9.
8. Ongaro C, Zanini A, Nastasi U, et al. Analysis of photoneutron spectra produced in medical accelerators. *Phys Med Biol* 2000;**45**:L55–61.
9. McGinley PH, Wood M, Mills M, Rodriguez R. Dose levels due to neutrons in the vicinity of high-energy medical accelerators. *Med Phys* 1976;**3**:397–402.
10. Akkurt I, Adler JO, Annand JR, et al. Photoneutron yields from tungsten in the energy range of the giant dipole resonance. *Phys Med Biol* 2003;**48**:3345–52.
11. Waller EJ, Jamieson TJ, Cole D, Cousins T, Jammal RB. Experimental and computational determination of neutron dose equivalent around radiotherapy accelerators. *Radiat Prot Dosim* 2003;**107**:225–32.
12. Allen PD, Chaudhri MA. Photoneutron production in tissue during high energy bremsstrahlung radiotherapy. *Phys Med Biol* 1988;**33**:1017–36.
13. Guo S, Ziemer PL. Health physics aspects of neutron activated components in a linear accelerator. *Health Phys* 2004;**86**:S94–102.
14. Swanson WP. Calculation of neutron yields released by electrons incident on selected materials. *Health Phys* 1978;**35**:353–67.
15. McCall RC, Hootman HE. Heavy metal shielding for neutron sources. *Health Phys* 1978;**35**:570–1.
16. Barquero R, Mendez R, Iniguez MP, Vega HR, Voytchev M. Thermoluminescence measurements of neutron dose around a medical linac. *Radiat Prot Dosim* 2002;**101**:493–6.
17. Becker J, Brunckhorst E, Schmidt R. Photoneutron production of a Siemens Primus linear accelerator studied by Monte Carlo methods and apaired magnesium and boron coated magnesium ionization chamber system. *Phys Med Biol* 2007;**52**:6375–87.
18. d'Errico F, Nath R, Tana L, Curzio G, Alberts WG. In-phantom dosimetryand spectrometry of photoneutrons from an 18 MeV linear accelerator. *Med Phys* 1998;**25**:1717–24.
19. d'Errico F, Luszik-Bhadra M, Nath R, Siebert BR, Wolf U. Depth dose-equivalent and effective energies of photoneutrons generated by 6–18 MeV X-ray beams for radiotherapy. *Health Phys* 2001;**80**:4–11.
20. Fernandez F, Domingo C, Amgarou K, et al. Neutron measurements in a Varian 2100 C LINAC facility using a Bonner sphere system based on passive gold activation detectors. *Radiat Prot Dosim* 2007;**126**:361–5.
21. Followill DS, Stovall MS, Kry SF, Ibbott GS. Neutron source strength measurements for Varian, Siemens, Elekta, and General Electric linear accelerators. *J Appl Clin Med Phys* 2003;**4**:189–94.

22. Ghiasi H, Mesbahi A. A new analytical formula for neutron capture gamma dose calculations in double-bend mazes in radiation therapy. *Rep Pract Oncol Radiother* 2012;**17**: 220–5.
23. Ghiasi H, Mesbahi A. Sensitization of the analytical methods for photoneutron calculations to the wall concrete composition in radiation therapy. *Rad Meas* 2012;**46**: 1–464.
24. Golnik N, Kaminski P, Zielczynski M. A measuring system with a recombination chamber for neutron dosimetry around medical accelerators. *Radiat Prot Dosim* 2004;**110**:273–6.
25. Naseri A, Mesbahi A. A review on photoneutrons characteristics in radiation therapy with high-energy photon beams. *Rep Pract Oncol Radiother* 2010;**15**:138–44.
26. Kase KR, Nelson WR, Fasso A, et al. Measurements of accelerator-produced leakage neutron and photon transmission through concrete. *Health Phys* 2003;**84**:180–7.
27. Jaradat AK, Biggs PJ. Measurement of the neutron leakage from a dedicated intraoperative radiation therapy electron linear accelerator and a conventional linearaccelerator for 9, 12, 15, 16, and 18(20) MeV electron energies. *Med Phys* 2008;**35**:1711–7.